ACS APPLIED MATERIALS & INTERFACES

Research Article

www.acsami.org

Composite Counter Electrode Based on Nanoparticulate PbS and Carbon Black: Towards Quantum Dot-Sensitized Solar Cells with Both High Efficiency and Stability

Yueyong Yang, Lifeng Zhu, Huicheng Sun, Xiaoming Huang, Yanhong Luo, Dongmei Li, and Qingbo Meng*

Key Laboratory for Renewable Energy, Chinese Academy of Sciences; Beijing Key Laboratory for New Energy Materials and Devices; Institute of Physics, Chinese Academy of Sciences, Beijing, 100190, People's Republic of China

ABSTRACT: PbS/carbon black (CB) composite counter electrode (CE) has been fabricated by a low cost and low temperature processable method using the wet chemistry synthesized PbS nanoparticles. The nanosized PbS in the composite CE provides a large area of catalytic sites, and the chain-type CB framework acts as an excellent electrical tunnel for fast electron transport from an external circuit to highly catalytic PbS nanoparticles. The optimized PbS/CB composite CE shows a charge transfer resistance (R_{CT}) as low as 10.28 Ω cm^2, which is an order of magnitude lower than the value obtained in the previous study on pure PbS CE. The CdS/CdSe quantum dot-sensitized solar cells with the PbS/CB composite CE achieve a photovoltaic conversion efficiency of 3.91% and no degradation of the efficiency over 1000 h under room conditions.

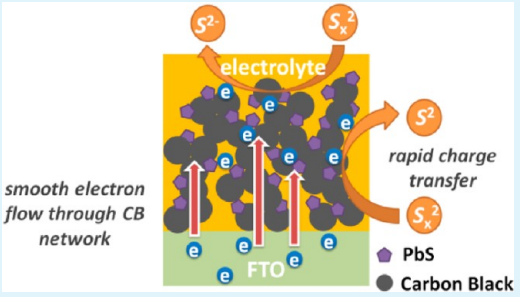

KEYWORDS: *quantum dot-sensitized solar cell, lead sulfide, carbon black, counter electrode, solvothermal, nanoparticle*

1. INTRODUCTION

Recently, quantum dot-sensitized solar cells (QDSCs) have attracted much attention. Compared with traditional dyes used in dye-sensitized solar cells (DSCs), the unique advantages of the use of quantum dots (QDs) as photon harvesters include strong photo-response in the visible region, easily tunable bandgap, and the expectation to obtain high efficiency by utilizing multiple exciton generation of QDs.[1−3] In the past few years, extensive efforts have been devoted to improve the performance of QDSCs, many of which focused on the improvement and modification of the photoelectrode, such as design and optimization of QD deposition methods on TiO_2 film,[4−10] optimization of TiO_2 film structure,[11−15] and employing new kinds of quantum dot sensitizers.[16−20] An impressive efficiency of up to 5.4% has been achieved with Mn-doped CdS/CdSe QD-sensitized photoanodes recently.[7] Except for the optimization of photoanodes, careful selection of the counter electrode (CE) as well as the electrolyte is also an equally important path to improve the performance of QDSCs. The widely used Pt CE for DSCs exhibits poor catalytic activity in QDSCs, resulting in a bottleneck for the electron flow. For most highly efficient QDSCs reported, Cu_2S was employed as the CE, showing outstanding catalytic activity and good electrical properties.[4,13,21−24] However, one of the key issues in QDSCs is the stability of the CE. It has been proved that brass based Cu_2S CE cannot stand the continuing corrosion in polysulfide electrolyte.[25] To overcome the limitations of the CE and improve the cell performance, the development of novel CEs for QDSCs has received much attention, such as Au,[9] CuS,[20,26] CoS,[27] conducting polymer,[28] and carbon materials.[29−31]

Among all these materials, PbS shows promising stability as well as good catalytic activity. Zaban et al. prepared PbS CE directly on Pb foil.[32] A charge transfer resistance (R_{CT}) of 130 Ω cm^2 was achieved, and the CdS/CdSe QDSCs based on such CE obtained an efficiency of 3.01%. This CE showed quite good stability over 100 h in a closed Teflon cell. These results suggest that PbS is a prospective catalyst that can be applied as highly performed CE in QDSCs. However, some issues of the PbS CE still have to be solved before it becomes competitive enough: (1) the R_{CT} value is too large compared with the ∼10 Ω cm^2 value of other metal sulfides like CoS; (2) the long-term stability of the Pb foil based CE is still questioned due to the slow reaction between Pb foil and alkalic polysulfide electrolyte, and (3) the utilization of metal foil based CEs is unsatisfactory, especially for cell sealing and large-scale fabrication. Therefore, it is of cardinal significance to develop new ways to overcome the current challenges of PbS CEs.

In this paper, we report a low cost and low-temperature processable PbS/carbon black (CB) composite CE for highly efficient CdS/CdSe QDSCs. PbS nanoparticles were synthesized through wet-chemistry, which enables mass production of electrode materials and facile fabrication of the electrode. A proper amount of CB was mixed with the PbS nanoparticles to

Received: August 25, 2012
Accepted: October 17, 2012
Published: October 17, 2012

   dx.doi.org/10.1021/am301787q | ACS Appl. Mater. Interfaces 2012, 4, 6162−6168

strengthen the bonding inside the film. The nanosized PbS particles in the PbS/CB composite CE provide a large area of catalytic sites, and the CB framework acts as an excellent electrical tunnel for fast electron transport from external circuit to highly catalytic PbS nanoparticles. The PbS/CB composite film shows outstanding electrocatalytic activity as well as unsurpassed stability in the polysulfide electrolytes. An improved efficiency of 3.91% has been obtained for the CdS/CdSe QDSCs using the optimized PbS/CB composite CEs.

2. EXPERIMENTAL SECTION

Preparation of PbS/CB Composite Counter Electrode. A 0.06 M $Pb(Ac)_2$ and 0.06 M thioacetamide solution with ethylenediamine as the solvent was prepared separately, mixed, and then heated at 60 °C in a sealed Teflon-lined autoclave for 5 h to obtain PbS powder.[33] The powders were washed with deionized water and ethanol each for three times and then dried in vacuum oven at room temperature for 12 h. A total weight of 2.2 g of PbS powder and CB with different ratios were mixed and subsequently added into polyvinylidene fluoride (PVDF) solution containing 0.2 g of PVDF as the binder and the proper amount of *N*-methyl pyrrolidone as the solvent. The mixture was placed in a ball mill working at 450 r/min for 4 h to form the pastes. The pastes were then coated on fluorine doped tin oxide (FTO) glass to give the film by doctor-blading. The PbS/CB composite CE was finally obtained by drying the film at 80 °C for an hour in the oven.

Preparation of Photoanodes and QDSCs. FTO glass (Nippon Sheet Glass; sheet resistance: 15 Ω/square) was first washed with mild detergent, subsequently rinsed with the water for several times and with ethanol in an ultrasonic bath, and finally dried under air stream. The preparation of 20 nm-sized anatase TiO_2 nanoparticles and TiO_2 paste were carried out according to the literature.[34] TiO_2 film (20 nm TiO_2 particles) with thickness of 10 μm, followed by another 5 μm scattering layer (300 nm TiO_2 particles) for the QD deposition, was prepared on FTOs using the screen printing technique. After printing, the films were heated at 80 °C for 30 min and finally sintered at 450 °C for 30 min. They were subsequently placed in 30 mM $TiCl_4$ aqueous solution at 70 °C for 40 min and then sintered at 500 °C for 30 min.

The chemical bath deposition (CBD) technique was employed to fabricate CdS and CdSe QDs in the sequence on the photoanodes.[35] All the QD (CdS and CdSe) depositions were kept at 10 °C. CdS was deposited with an aqueous solution with the composition of 20 mM $CdCl_2$, 66 mM NH_4Cl, 140 mM thiourea, and 230 mM ammonia with a final pH ca. 9.5 for 40 min. The films were washed with water completely. Subsequently, CdSe was deposited by mixing an aqueous solution with 26 mM $CdSO_4$, 40 mM $N(CH_2COONa)_3$, and 26 mM Na_2SeSO_3. The CdSe deposition was maintained for 5.5 h. At last, the photoanodes were passivated with ZnS by twice dipping into 0.1 M $Zn(CH_3COO)_2$ and Na_2S aqueous solution for 1 min alternately.

The QD-sensitized photoanode and CE were clamped together with a spacer and polysulfide electrolyte (2 M Na_2S and 2 M S aqueous solution) filled between them to form the QDSC. A mask with a window of 0.15 cm^2 was clipped on the photoanode to define the active area of the cell. As to QDSCs for stability tests, pre-prepared QD-sensitized photoanodes and CEs were sealed with ethylene-vinyl acetate (EVA) copolymer thin film under hot press.

Characterization. The cells were irradiated by an Oriel Solar Simulator 91192 under AM 1.5 100 mW/cm^2. Princeton Applied Research, Model 263 A was used to record the *J*−*V* characteristics of the cells. Electrochemical impedance spectroscopy (EIS) measurements were performed with an IM6ex electrochemical workstation (ZAHNER) in the frequency range between 0.1 and 10^5 Hz. The magnitude of alternative signal was 10 mV. The thickness of PbS and TiO_2 films were measured by a profiler (KLA-tencor). The morphology of the PbS particles and CEs was observed by a scanning electron microscope (SEM, FEI XL30 S-FEG). X-ray diffraction (XRD) measurement (M18X-AHF, MAC Science) was employed to characterize PbS powder.

3. RESULTS AND DISCUSSION

In QDSCs, the S_x^{2-} in the electrolyte is continually reduced to S^{2-} at the CE side. The charge transfer rate at the electrolyte/CE interface is greatly affected by the number of the reaction sites on CEs, which means the surface morphology is one of the most important factors influencing the performance of the CE. For the PbS/CB composite CE fabricated by our method, the sizes of the pre-synthesized PbS particles directly determine the surface area of the CE. Thus, characterization of the pre-prepared PbS particles was first conducted. The black powder synthesized from solvothermal reaction was characterized by XRD (Figure 1). The peaks of corresponding crystal planes are

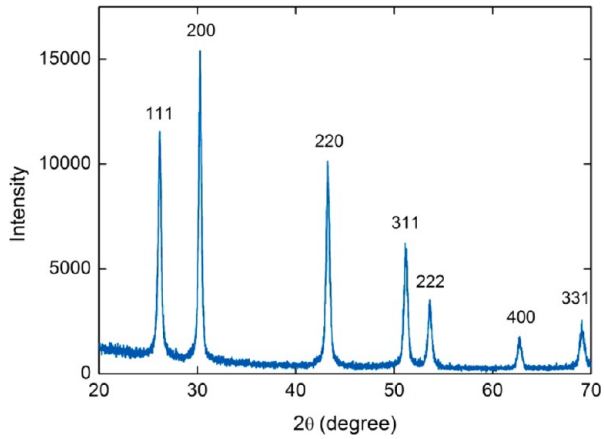

Figure 1. XRD spectra of the PbS powder synthesized from solvothermal reaction.

indexed in the figure, matching very well to the cubic phase PbS (JCPDS card No. 05-0592). The SEM image of the PbS powder and CB nanoparticles can be seen in Figure 2a,b, respectively. Most of the PbS nanoparticles synthesized are around 20 nm, while most CB particles have a size around 50 nm. Figure 2c shows the SEM image of the surface morphology of PbS/CB composite CE. The microstructure of smaller PbS nanoparticles adhered on CB framework can be clearly observed. The CB framework, together with small PbS particles, ensures the large surface area of PbS/CB composite CE, providing enough reaction sites for the catalytic reduction of S_x^{2-}.

Our previous study has already confirmed that CB can improve the conductivity of the CE, while CB itself is not highly catalytic in QDSCs.[23] In order to figure out the influence of CB ratio on the performance of PbS/CB composite CEs, four kinds of PbS/CB composite paste with different CB compositions were prepared, in which the weight ratio of PbS and CB is 21:1 (Sample B), 10:1 (Sample C), 5:1 (Sample D), and 1:1 (Sample E), respectively. Paste without CB (Sample A) and pure CB were also prepared as the reference. The content of PVDF among the solid mixture was kept constant at 1/12 weight ratio for all pastes. The thicknesses of PbS based films fabricated from different pastes, which are shown in Table 1, were controlled by adjusting the amount of *N*-methyl pyrrolidone solvent in the paste. Samples A, B, C, and D show quite close thickness between 3.0 and 3.9 μm. For Sample E and pure CB CE, the films are thicker than other samples due

dx.doi.org/10.1021/am301787q | ACS Appl. Mater. Interfaces 2012, 4, 6162−6168

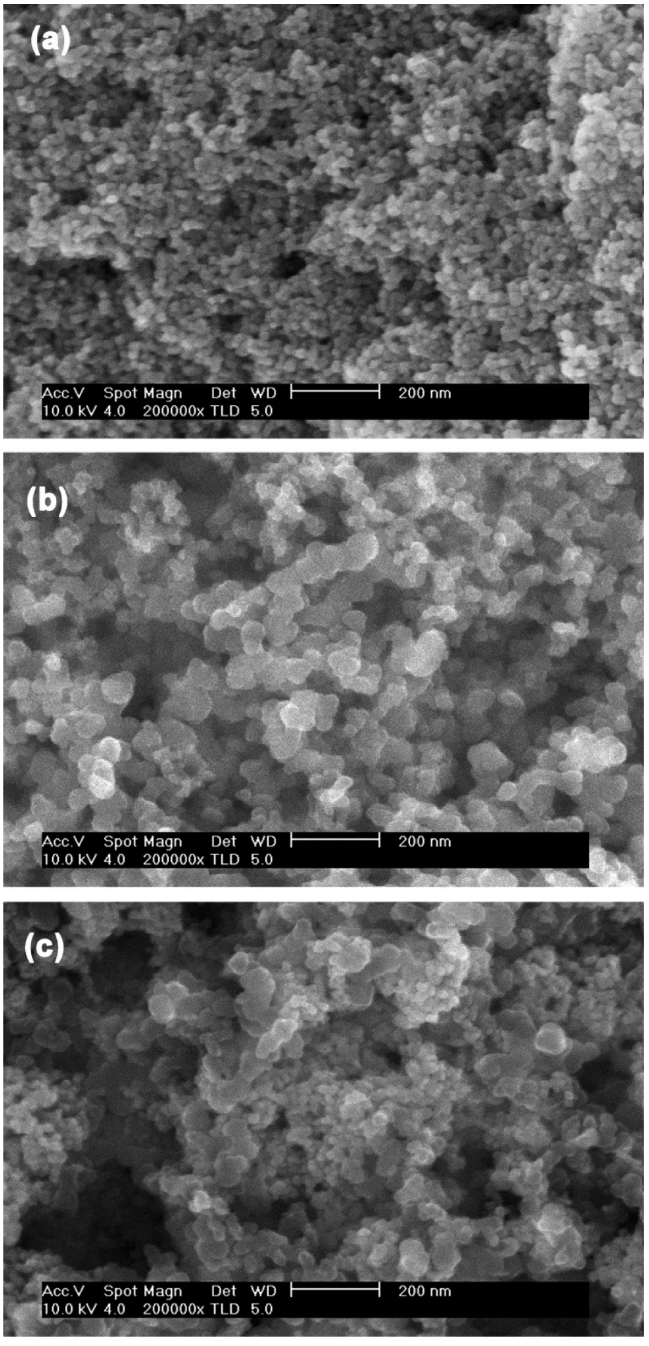

Figure 2. (a) SEM image of the pre-prepared PbS nanoparticles. (b) SEM image of the CB nanoparticles. (c) Surface of PbS/CB composite CE (the mass ratio of PbS and CB was 10:1).

Table 1. Thickness of CE Films Fabricated from Different Pastes

CE sample	PbS/CB (w/w)	film thickness (μm)
A	pure PbS	3.0
B	21:1	3.5
C	10:1	3.9
D	5:1	3.4
E	1:1	5.7
pure CB		11.0
Cu_2S		4.1

to the larger viscosity of the pastes. The adherence of all kinds of films on FTO glass is good. However, we find that the internal bonding of the PbS/CB composite films is better than the pure PbS films. When removing the films from the FTO substrates with violent force, the PbS/CB composite films tend to remain as a whole, while pure PbS films often crack into many small pieces. For comparison, screen-printed Cu_2S CE on FTO with thickness of 4.1 μm was also prepared on the basis of our previous work.[23]

Electrochemical impedance spectroscopy (EIS) measurements, which are widely used in characterizing sensitized solar cells,[36−39] have been carried out to investigate the charge transfer process between PbS/CB composite CE and the polysulfide electrolyte. Thin-layer sandwiched cells with two symmetric CEs placed face to face were fabricated for EIS measurements. The area of Pt CE is 0.502 cm^2. The area of all the other CEs is 0.4 cm^2. The distance between the CEs was kept constant by a spacer. Aqueous solution with 2 M Na_2S and 2 M S was used as the electrolyte. The Nyquist plots of different PbS based CEs and Pt CE are presented in Figure 3b,c. At the high frequencies around 100 kHz, the sheet resistance of the CE can be determined. For our CEs, the first high-frequency semicircle in the Nyquist plots between 10 and 100 kHz is possibly related to the solid−solid interface (R_{CT1}).[40] In the frequency range between 100 Hz and 10 kHz, the impedance was associated with the electron transfer at the CE/electrolyte interface, which consists of the charge transfer resistance (R_{CT2}) and the double layer capacitance (CPE, constant phase element).[41] The plots are fitted with the equivalent circuit shown in Figure 3a, and the fitting results are shown in Table 2. The Pt CE and pure CB CE give unsatisfying R_{CT2} values up to several hundred Ω cm^2, suggesting that their catalytic activity is very poor in polysulfide electrolyte. The R_{CT2} value of Sample A is 120.36 Ω cm^2, which is very close to the R_{CT} value of PbS CE reported in the previous study.[32] Samples B, C, and D show quite similar low R_{CT2} values. Sample C, with 10:1 weight ratio of PbS and CB, exhibits the lowest R_{CT2} value of 10.28 Ω cm^2, which is an order of magnitude lower than the R_{CT2} value of the pure PbS CE, suggesting that CB greatly enhances the charge transfer of the PbS/CB composite CEs. The differences between the PbS/CB composite CEs and pure PbS CEs are likely related to the strength of bonding between nanoparticles within the film, which can be implied from their mechanical properties mentioned above. In the pure PbS CE, the poor connections between the PbS nanoparticles may create a bottleneck for the electrons flowing from the external circuit to transport to the PbS/electrolyte interface. This means that catalytic sites on PbS nanoparticles may not be fully utilized, thus resulting in a higher overall R_{CT2} value. As for the PbS/CB composite CEs, the CB particles have good connections with the PbS nanoparticles, creating a framework that tightly holds the PbS nanoparticles (Scheme 1). The botryoidal chains of CB particles serve as the excellent tunnels for the electron transport and thus significantly reduce the internal resistance of the CE film, which ensures the full utilization of highly catalytic PbS nanoparticles. On the other hand, though proper amount of CB in PbS/CB composite film can improve the performance of CE, excessive CB will reduce the amount of highly catalytic sites of PbS in the CE and lead to a higher R_{CT2} value of Sample E up to 70.30 Ω cm^2. The screen-printed Cu_2S CE exhibits a quite low R_{CT2} value, which is 7.44 Ω cm^2 lower than that of the optimized PbS/CB composite CE.

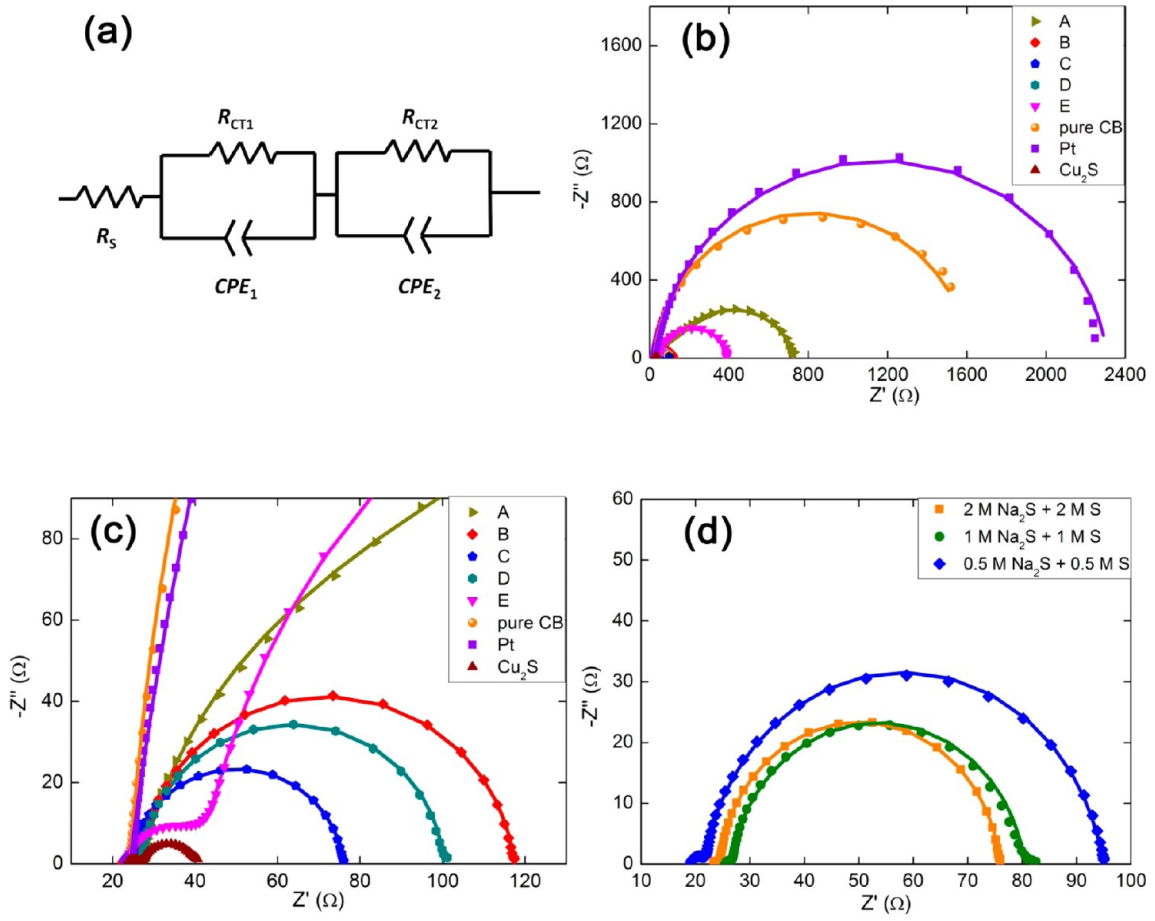

Figure 3. (a) Equivalent circuit for fitting EIS. R_S: sheet resistance of the CE; R_{CT1}: charge transfer resistance of solid/solid interface; R_{CT2}: charge transfer resistance of electrolyte/CE interface; CPE: constant phase element of electrical double layer. (b) Nyquist plots of symmetric thin-layer sandwich-type cells with different kinds of PbS based CEs, Pt CE, screen-printed Cu_2S CE, and pure CB CE measured at zero bias potential. (c) Magnified plots of (b). (d) Nyquist plots of symmetric thin-layer sandwich-type cells (Sample C) with different kinds of electrolyte. The area of Pt CE is 0.502 cm^2. The area of all the other CEs for testing is 0.4 cm^2. The distance between the CEs placed face to face is kept constant by a spacer. The dots are the experimental data, and the lines are the fitted curves.

Table 2. Fitted Impedance Values of Various CEs with Electrolyte Containing 2 M Na_2S and 2 M S

CE samples	A	B	C	D	E	Pt	pure CB	Cu_2S
R_S (Ω)	13.56	11.11	11.52	12.53	11.66	11.49	11.48	11.82
R_{CT1} (Ω cm^2)	20.40	0.88	0.29	0.40	3.88	0.29	0.28	0.59
R_{CT2} (Ω cm^2)	120.36	18.13	10.28	14.64	70.30	574.99	315.60	2.84

We further investigated the performance of PbS/CB composite CE in electrolytes with different polysulfide concentrations. The resulting Nyquist plots are presented in Figure 3d. Specific fitted R_{CT2} values are shown in Table 3. The R_{CT2} value of Sample C is already as low as 14.63 Ω cm^2 in the electrolyte of 0.5 M Na_2S and 0.5 M S, suggesting that PbS itself a good electroactive material even in low concentrated polysulfide electrolyte. An obvious decrease of R_{CT2} values are observed with increasing polysulfide concentration. The lowest R_{CT2} value of 10.28 Ω cm^2 occurs with the electrolyte of 2 M Na_2S and 2 M S. Higher concentration of the electroactive species of polysulfide at the CE surface is responsible for the enhancement of the charge transfer rate. The $J-V$ curves of QDSCs based on PbS/CB composite CE (Sample C) with different types of polysulfide electrolyte are presented in Figure 4a. Detailed data are shown in Table 4. A quite high efficiency of 3.28% can already be achieved with the electrolyte containing 0.5 M Na_2S and 0.5 M S. Cells with higher concentrated polysulfide electrolyte give better performance, which is consistent with the phenomenon mentioned in the previous study.[42] The highest efficiency of 3.91% is obtained with the electrolyte of 2 M Na_2S and 2 M S.

The $J-V$ characteristics of the QDSC employing different PbS/CB composite CEs along with TiO_2/CdS/CdSe photoanode were evaluated. Aqueous solution containing 2 M Na_2S and 2 M S was used as the electrolyte. QDSCs with bright Pt, pure PbS CE, pure CB CE, and screen-printed Cu_2S CE were also tested as the reference. The $J-V$ curves of these cells tested under AM 1.5 100 mW/cm^2 are shown in Figure 4b. Detailed data are presented in Table 5. Cells with Pt CE and pure CB CE show quite poor performance, due to the low catalytic activity of these CEs in polysulfide electrolyte. An efficiency of 3.06% was achieved by QDSCs with Sample A, which contained no CB. Very close improved performances over

dx.doi.org/10.1021/am301787q | ACS Appl. Mater. Interfaces 2012, 4, 6162−6168

Scheme 1. Scheme of the Structure of PbS/CB Composite CE[a]

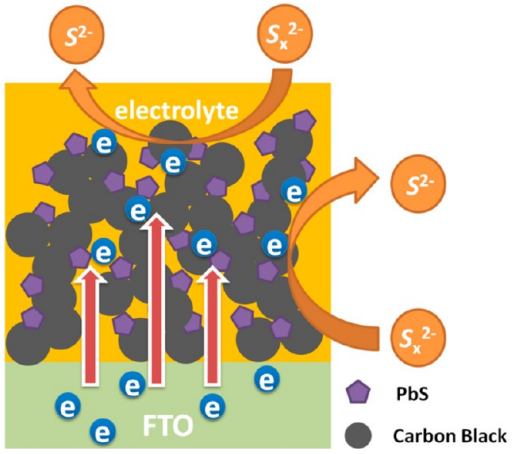

[a]The chain-type CB (big grey spheres) aggregates form a framework that tightly holds the PbS nanoparticles (small purple pentagons). Electrons coming from the external circuit can transport smoothly to the highly catalytic reaction sites on PbS, thus overcoming the bottleneck of poor connections between PbS nanoparticles.

Sample A were achieved by Samples B, C, and D. Consistent with the results of EIS measurements, the QDSCs with these three kinds of samples exhibit a significant increase in fill factor (FF) over Sample A, demonstrating the improvement of charge transfer and a reduction of internal resistance of QDSCs by the CB. The cell with Sample C achieved the highest efficiency among the cells with PbS based CEs (3.91%), which is just slightly lower than that with screen-printed Cu_2S CE (3.92%) due to the small absolute difference between the R_{CT2} values of these two CEs. The negative effect of excessive amount of CB can be confirmed by the obvious decrease of FF for QDSCs with Sample E, which contains an equal amount of CB and PbS in weight.

The CB framework together with PVDF binder provides good physical contact between nanoparticles and the FTO substrate, which has positive influence on the long-term stability of the PbS/CB composite CE. Limited by our testing equipment, a less rigorous but effective enough stability test has been carried out to observe whether the PbS/CB composite CE is stable in QDSCs. The sealed QDSCs with PbS/CB composite CE (Sample C) were kept in day−night room conditions for over 1000 h and measured under AM 1.5 100 mW/cm^2 illumination every day. The observed efficiency is shown in Figure 5. No degradation of efficiency is found over such a long time. The result clearly demonstrates much better stability of PbS/CB composite CE compared with the CE based on Cu_2S nanoparticles, whose efficiency falls to around 90% of its initial value after 7 days.[23]

4. CONCLUSIONS

Highly electrocatalytic and stable PbS/CB composite CEs have been fabricated using a low cost, low-temperature processable technique. A proper amount of CB was mixed with the

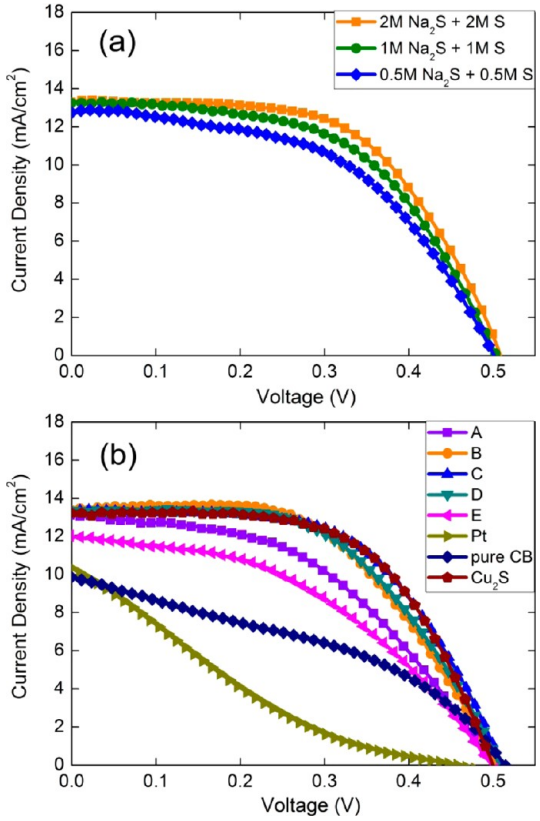

Figure 4. (a) J−V characteristics of QDSCs based on PbS/CB composite CE (Sample C) with different types of polysulfide electrolyte. (b) J−V characteristics of QDSCs with different CEs under AM 1.5 100 mW/cm^2 illumination. The electrolyte is 2 M Na_2S + 2 M S aqueous solution.

Table 4. Photovoltaic Properties of PbS/CB Composite CE Based CdS/CdSe QDSCs with Different Types of Electrolyte

electrolyte	J_{SC} (mA cm^{-2})	V_{OC} (mV)	FF	efficiency (%)
2 M Na_2S + 2 M S	13.32	509.58	0.58	3.91
1 M Na_2S + 1 M S	13.25	504.13	0.54	3.63
0.5M Na_2S + 0.5M S	12.75	501.60	0.51	3.28

Table 5. Photovoltaic Properties of CdS/CdSe QDSCs with Different CEs

CE sample	PbS/CB (w/w)	J_{SC} (mA cm^{-2})	V_{OC} (mV)	FF	efficiency (%)
A	pure PbS	13.09	500.50	0.47	3.06
B	21:1	13.37	504.38	0.55	3.70
C	10:1	13.32	509.58	0.58	3.91
D	5:1	13.36	507.50	0.55	3.71
E	1:1	11.98	497.50	0.44	2.63
Pt		10.32	457.53	0.18	0.85
pure CB		9.87	514.90	0.39	1.98
Cu_2S		13.23	499.33	0.59	3.92

Table 3. Fitted R_{CT2} Values of PbS/CB Composite CE Sample C in Various Electrolytes

electrolyte	0.5 M Na_2S + 0.5 M S	1 M Na_2S + 1 M S	2 M Na_2S + 2 M S
R_{CT2} (Ω cm^2)	14.63	10.79	10.28

dx.doi.org/10.1021/am301787q | ACS Appl. Mater. Interfaces 2012, 4, 6162−6168

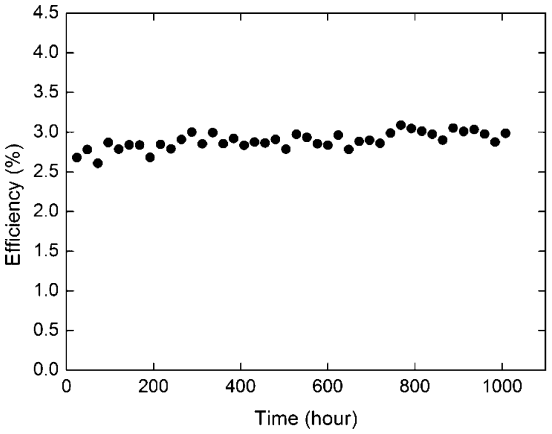

Figure 5. Efficiency test of PbS/CB composite CE based sealed QDSCs over 1000 h. The cells are kept in room conditions and measured under AM 1.5 100 mW/cm^2 illumination every day.

nanoparticulate PbS pre-synthesized by a solvothermal process to strengthen the bonding inside the film, improving both mechanical strength and electrical conductivity. PbS/CB composite CEs with various CB ratios have been systematically studied by EIS and *J*−*V* measurements. When the weight ratio of PbS and CB was 10:1, QDSC with the PbS/CB composite CE achieves the optimized efficiency up to 3.91%. The PbS/CB composite CE exhibits the lowest R_{CT2} value of 10.28 Ω cm^2, which is an order lower than the value in the previous study. The stability test of sealed QDSCs with PbS/CB composite CEs over 1000 h proves that the PbS/CB composite CEs are highly stable working in the QDSCs. These results show the promising application prospect of PbS/CB composite film as the CE in QDSCs.

AUTHOR INFORMATION

Corresponding Author

*Tel./Fax: +86-10-8264-9242. E-mail: qbmeng@iphy.ac.cn.

Notes

The authors declare no competing financial interest.

ACKNOWLEDGMENTS

The authors appreciate the financial support of National Key Basic Research Program (973 project, No. 2012CB932903), National Natural Science Foundation of China (Nos. 20725311, 51072221, and 21173260), and the Knowledge Innovation Program of the Chinese Academy of Sciences (No. KJCX2-YW-W27).

REFERENCES

(1) Nozik, A. J. *Phys. E* **2002**, *14*, 115−120.
(2) Kamat, P. V. *J. Phys. Chem. C* **2008**, *112*, 18737−18753.
(3) Yang, Z. S.; Chen, C. Y.; Roy, P.; Chang, H. T. *Chem. Commun.* **2011**, *47*, 9561−9571.
(4) Giménez, S.; Mora-Seró, I.; Macor, L.; Guijarro, N.; Lana-Villarreal, T.; Gómez, R.; Diguna, L. J.; Shen, Q.; Toyoda, T.; Bisquert, J. *Nanotechnology* **2009**, *20*, 295204.
(5) Lin, S. C.; Lee, Y. L.; Chang, C. H.; Shen, Y. J.; Yang, Y. M. *Appl. Phys. Lett.* **2007**, *90*, 143517.
(6) Robel, I.; Subramanian, V.; Kuno, M.; Kamat, P. V. *J. Am. Chem. Soc.* **2006**, *128*, 2385−2393.
(7) Santra, P. K.; Kamat, P. V. *J. Am. Chem. Soc.* **2012**, *134*, 2508−2511.
(8) Lee, H.; Wang, M. K.; Chen, P.; Gamelin, D. R.; Zakeeruddin, S. M.; Grätzel, M.; Nazeeruddin, M. K. *Nano Lett.* **2009**, *9*, 4221−4227.
(9) Chong, L. W.; Chien, H. T.; Lee, Y. L. *J. Power Sources* **2010**, *195*, 5109−5113.
(10) Lee, Y. H.; Im, S. H.; Rhee, J. H.; Lee, J. H.; Il Seok, S. *ACS Appl. Mater. Interfaces* **2010**, *2*, 1648−1652.
(11) Lee, W.; Kang, S. H.; Kim, J. Y.; Kolekar, G. B.; Sung, Y. E.; Han, S. H. *Nanotechnology* **2009**, *20*, 335706.
(12) Lee, W.; Kang, S. H.; Min, S. K.; Sung, Y. E.; Han, S. H. *Electrochem. Commun.* **2008**, *10*, 1579−1582.
(13) Shen, Q.; Yamada, A.; Tamura, S.; Toyoda, T. *Appl. Phys. Lett.* **2010**, *97*, 123107.
(14) Zhang, Q. X.; Guo, X. Z.; Huang, X. M.; Huang, S. Q.; Li, D. M.; Luo, Y. H.; Shen, Q.; Toyoda, T.; Meng, Q. B. *Phys. Chem. Chem. Phys.* **2011**, *13*, 4659−4667.
(15) Zhang, Q. X.; Chen, G. P.; Yang, Y. Y.; Shen, X.; Zhang, Y. D.; Li, C. H.; Yu, R. C.; Luo, Y. H.; Li, D. M.; Meng, Q. B. *Phys. Chem. Chem. Phys.* **2012**, *14*, 6479−6486.
(16) Lee, H.; Leventis, H. C.; Moon, S. J.; Chen, P.; Ito, S.; Haque, S. A.; Torres, T.; Nuesch, F.; Geiger, T.; Zakeeruddin, S. M.; Grätzel, M.; Nazeeruddin, M. K. *Adv. Funct. Mater.* **2009**, *19*, 2735−2742.
(17) Hu, X.; Zhang, Q. X.; Huang, X. M.; Li, D. M.; Luo, Y. H.; Meng, Q. B. *J. Mater. Chem.* **2011**, *21*, 15903−15905.
(18) Yu, P. R.; Zhu, K.; Norman, A. G.; Ferrere, S.; Frank, A. J.; Nozik, A. J. *J. Phys. Chem. B* **2006**, *110*, 25451−25454.
(19) Braga, A.; Giménez, S.; Concina, I.; Vomiero, A.; Mora-Seró, I. *J. Phys. Chem. Lett.* **2011**, *2*, 454−460.
(20) Li, T. L.; Lee, Y. L.; Teng, H. *Energy Environ. Sci.* **2012**, *5*, 5315−5324.
(21) Huang, S. Q.; Zhang, Q. X.; Huang, X. M.; Guo, X. Z.; Deng, M. H.; Li, D. M.; Luo, Y. H.; Shen, Q.; Toyoda, T.; Meng, Q. B. *Nanotechnology* **2010**, *21*, 375201.
(22) Deng, M. H.; Zhang, Q. X.; Huang, S. Q.; Li, D. M.; Luo, Y. H.; Shen, Q.; Toyoda, T.; Meng, Q. B. *Nanoscale Res. Lett.* **2010**, *5*, 986−990.
(23) Deng, M. H.; Huang, S. Q.; Zhang, Q. X.; Li, D. M.; Luo, Y. H.; Shen, Q.; Toyoda, T.; Meng, Q. B. *Chem. Lett.* **2010**, *39*, 1168−1170.
(24) Hossain, M. A.; Jennings, J. R.; Shen, C.; Pan, J. H.; Koh, Z. Y.; Mathews, N.; Wang, Q. *J. Mater. Chem.* **2012**, *22*, 16235−16242.
(25) Radich, J. G.; Dwyer, R.; Kamat, P. V. *J. Phys. Chem. Lett.* **2011**, *2*, 2453−2460.
(26) Yang, Z. S.; Chen, C. Y.; Liu, C. W.; Li, C. L.; Chang, H. T. *Adv. Energy Mater.* **2011**, *1*, 259−264.
(27) Yang, Z. S.; Chen, C. Y.; Liu, C. W.; Chang, H. T. *Chem. Commun.* **2010**, *46*, 5485−5487.
(28) Yeh, M. H.; Lee, C. P.; Chou, C. Y.; Lin, L. Y.; Wei, H. Y.; Chu, C. W.; Vittal, R.; Ho, K. C. *Electrochim. Acta* **2011**, *57*, 277−284.
(29) Zhang, Q. X.; Zhang, Y. D.; Huang, S. Q.; Huang, X. M.; Luo, Y. H.; Meng, Q. B.; Li, D. M. *Electrochem. Commun.* **2010**, *12*, 327−330.
(30) Fan, S. Q.; Fang, B.; Kim, J. H.; Kim, J. J.; Yu, J. S.; Ko, J. *Appl. Phys. Lett.* **2010**, *96*, 063501.
(31) Seol, M.; Ramasamy, E.; Lee, J.; Yong, K. *J. Phys. Chem. C* **2011**, *115*, 22018−22024.
(32) Tachan, Z.; Shalom, M.; Hod, I.; Rühle, S.; Tirosh, S.; Zaban, A. *J. Phys. Chem. C* **2011**, *115*, 6162−6166.
(33) Chu, H. B.; Chen, G. D.; Li, X. M.; Li, Y. *Chin. J. Inorg. Chem.* **2004**, *20*, 1177−1181.
(34) Li, D. M.; Wang, M. Y.; Wu, J. F.; Zhang, Q. X.; Luo, Y. H.; Yu, Z. X.; Meng, Q. B.; Wu, Z. J. *Langmuir* **2009**, *25*, 4808−4814.
(35) Niitsoo, O.; Sarkar, S. K.; Pejoux, C.; Rühle, S.; Cahen, D.; Hodes, G. *J. Photochem. Photobiol., A* **2006**, *181*, 306−313.
(36) Wang, Q.; Moser, J. E.; Grätzel, M. *J. Phys. Chem. B* **2005**, *109*, 14945−14953.
(37) Wang, Q.; Ito, S.; Grätzel, M.; Fabregat-Santiago, F.; Mora-Seró, I.; Bisquert, J.; Bessho, T.; Imai, H. *J. Phys. Chem. B* **2006**, *110*, 25210−25221.
(38) González-Pedro, V.; Xu, X. Q.; Mora-Seró, I.; Bisquert, J. *ACS Nano* **2010**, *4*, 5783−5790.
(39) Han, L. Y.; Koide, N.; Chiba, Y.; Islam, A.; Komiya, R.; Fuke, N.; Fukui, A.; Yamanaka, R. *Appl. Phys. Lett.* **2005**, *86*, 213501.

(40) Murakami, T. N.; Ito, S.; Wang, Q.; Nazeeruddin, M. K.; Bessho, T.; Cesar, I.; Liska, P.; Humphry-Baker, R.; Comte, P.; Péchy, P.; Grätzel, M. *J. Electrochem. Soc.* **2006**, *153*, A2255−A2261.
(41) Hauch, A.; Georg, A. *Electrochim. Acta* **2001**, *46*, 3457−3466.
(42) Hodes, G.; Manassen, J.; Cahen, D. *J. Electrochem. Soc.* **1980**, *127*, 544−549.